Removal of Aqueous Cr(VI) by a Combination of Photocatalytic Reduction and Coprecipitation

Xiaoling Wang, S. O. Pehkonen, and Ajay K. Ray*

Department of Chemical and Environmental Engineering, National University of Singapore, 10 Kent Ridge Crescent, Singapore 119260, Singapore

Semiconductor photocatalytic reduction is a relatively new technique for the removal of dissolved toxic metal ions from wastewater. In this paper, adsorption and photocatalytic reduction of Cr(VI) to Cr(III) inaqueous solutions by UV/TiO_2 photocatalysis has been investigated. It has been observed that the pH of the solution plays an important role in this reaction. An acidic medium is favorable for Cr(VI) photocatalytic reduction, where 94% of Cr(VI) was photoreduced within 1 h at pH 3 when 2 g/L of TiO_2 was used as the slurry. An adsorption study shows that the photocatalytic reduction mainly occurs on the surface of TiO_2. The presence of Fe(III) improved the photocatalytic reduction of Cr(VI) because it was observed that an additional reaction between Fe(II) and Cr(VI) takes place in the UV/TiO_2 reduction process. A new combination of photocatalytic reduction and metal ion coprecipitation using $Fe(OH)_3$ for complete removal of aqueous Cr [Cr(VI) as well as Cr(III)] was designed, which reduced the chromium concentration from 30 ppm to 17 ppb for a simulated wastewater. Thermodynamic analysis showed that TiO_2 cannot photoreduce Cr(III) to Cr(0), but reduction is possible with ZnS. When kinetic experiments were performed, it was observed that more than 86% of Cr(III) could be photoreduced to Cr(0) in 5 h with a ZnS catalyst.

Introduction

The interest in the application of semiconductor photocatalysis for wastewater treatment has grown exponentially over the past 10 years.[1] This technology is based on the reactive electrons and holes generated on the surface of a semiconductor when it is illuminated by light with energy greater than its band-gap energy. These electrons and holes either recombine or become involved in redox reactions. Any species with a reduction potential more positive than that of the conduction band of the semiconductor can consume electrons, while any species with an oxidation potential more negative than that of the valence band can consume the holes to complete the redox reaction cycle. Several metal oxide and sulfide semiconductors can be used to promote a wide range of chemical reactions because they have suitable band-gap energies, E_g. They include TiO_2 (E_g = 3.2 eV), ZnO (E_g = 3.2 eV), and ZnS (E_g = 3.6 eV). Among these semiconductors, TiO_2 is the most widely used photocatalyst because of its favorable chemical property, high stability, and low cost.[2] The band-gap energy of TiO_2 is 3.2 eV, equivalent to UV light of 380 nm, and therefore is photoexcited by near-UV illumination. The holes that are generated on TiO_2 are highly oxidizing, and there has been abundant literature on the utilization of TiO_2 in the oxidative degradation of organics. In addition to organics, the inorganic species with a reduction potential more positive than that of the conduction band of the semiconductor can consume the electrons and complete the redox reaction cycle. Recently, increasing attention has been paid to the photocatalytic reduction of inorganic contaminants. The application of the TiO_2 photocatalytic reduction process is reported to effectively remove various toxic metal ions, such as Hg(II),[3,4] Ag(I),[4] As(V)/As(III),[5,6] and Cr(VI).[3,7−12]

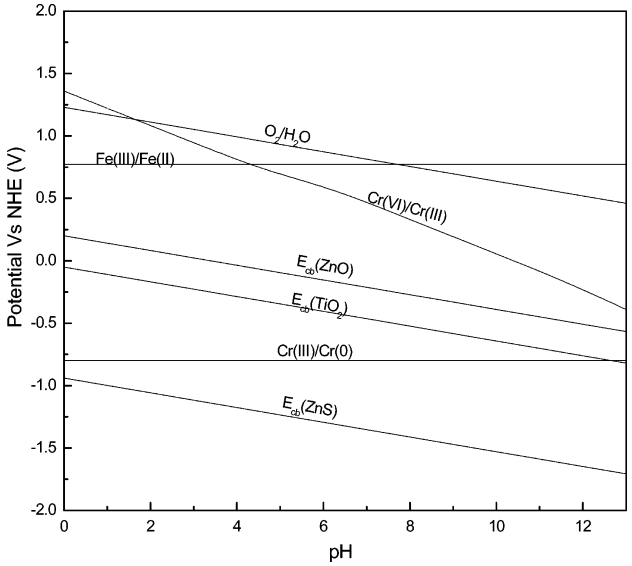

Figure 1. Energy level of the conduction band of semiconductors[16] and reduction potentials of relevant metal ions[17] as a function of pH.

Besides TiO_2, the application of ZnO[12−14] and CdS[15] in the photocatalytic reduction of Cr(VI) to Cr(III) has also been reported.

Figure 1 illustrates the position of the conduction band of various semiconductors as a function of pH. The figure is generated using data from the literature.[16,17] Comparing them with the reduction potentials of chromium in different forms, one can see that (a) Cr(VI) can be photocatalytically reduced to Cr(III) by most semiconductors, while only ZnS can photoreduce Cr(III) to Cr(0), (b) the reduction potential of Cr(VI) to Cr(III) is pH dependent, and the thermodynamic driving force for Cr(VI) reduction decreases with increasing pH, indicating that the photocatalytic reduction of Cr(VI) is favored at low pH, and (c) if Fe(III) or O_2 is present in the

* To whom correspondence should be addressed. Tel.: +65 6874 8049. Fax: +65 6779 1936. E-mail: cheakr@nus.edu.sg.

10.1021/ie030580j CCC: $27.50
Published on Web 03/03/2004

solution, they would compete with photoreduction of Cr(VI) because their reduction potentials are comparable. Although there are a number of studies on the photocatalytic reduction of Cr(VI) over semiconductor catalysts,[10−12] little information is reported related to coreactants except oxygen.[4,8] In this paper, a detailed investigation of the photocatalytic reduction of Cr(VI) in the presence of ferric ions and in the presence (and absence) of dissolved oxygen is presented.

Chromium is a typical component in many wastewaters, and there have been many studies to determine the effectiveness of water treatment processes in removing aqueous chromium ions. In these studies, the first step is always the conversion of Cr(VI) to Cr(III) by reducing agents, followed by the removal of Cr(III). Lime softening, alum coagulation, and iron coagulation (using ferric sulfate) have been found to be capable of removing Cr(III). Recently, the research focus has shifted to overcoming the limitations of the conventional pump-and-treat approach.[18] Photocatalytic treatment of Cr(VI) is a relatively new technology. However, the UV/TiO_2 photocatalysis can only reduce Cr(VI) to Cr(III), which is still toxic to humans. Hence, to achieve a nearly complete removal of chromium from water, a new combination of photocatalytic reduction and metal ion coprecipitation is proposed in this study. In this paper, we also report the photocatalytic reduction of Cr(III) using ZnS because Figure 1 clearly indicates that the reduction of Cr(III) to the elemental form is thermodynamically possible by ZnS.

Experimental Methods

TiO_2 Degussa P25 was used as the photocatalyst in most experiments. Some experiments were carried out using other semiconductors, such as ZnO (Aldrich Chemicals) and ZnS (Riedel-de Haen Chemicals). The Brunauer−Emmett−Teller specific surface areas of TiO_2, ZnO, and ZnS, measured by nitrogen adsorption at −196 °C, were found to be 43.8, 5.9, and 6.4 m^2/g, respectively. The following chemicals (all reagent grade) were also used: $K_2Cr_2O_7$ (Fluka Chemicals), $CrCl_3 \cdot 6H_2O$ (Sigma Chemicals), iron standard solution (BDH Chemicals), and formic acid and $Zn(NO_3)_2$ (Merck Inc.).

Experiments were carried out in a 200-mL cylindrical Teflon reactor at room temperature (295 ± 2 K). A 150-mL reaction mixture inside the reactor was maintained in suspension by a magnetic stirrer. The pH adjustments were made using dilute HNO_3 and NaOH. Irradiation was provided by a 450-W Xe arc lamp (Oriel model 6266) with a UV−vis band-pass filter (Oriel model 59450) placed on the top of the reactor. The light emission is above the wavelength of 290 nm, and the light intensity at the level of the reactor bottom was found to be about 22.0 W/m^2 between 290 and 400 nm measured using a UVI*tec* RX-003 radiometer. This light was employed as incident light in most experiments. In the experiment of lower light intensity, a neutral density filter (Oriel model 59680) was mounted on the band-pass filter. It can attenuate ∼58% of the incident light intensity. The experimental setup is shown in Figure 2, and a more detailed description can be found elsewhere.[19,20] In all of the photocatalysis experiments described below, formic acid is used to remove photogenerated holes in order to allow the redox reaction to continue. The concentration of formic acid in the reaction mixture was 20 mM in all experiments reported in this work because above this concentration no significant improvement in rate was observed. The suspensions are initially maintained under agitation in the dark for 60 min to allow for adsorption−desorption equilibrium to be established. During the irradiation, aliquots of the reaction solution were withdrawn intermittently.

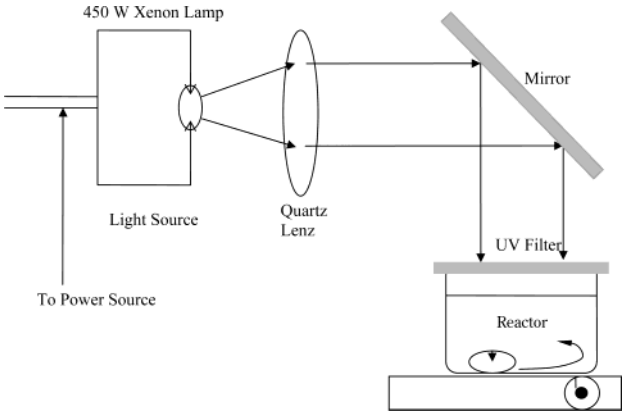

Figure 2. Experimental setup.

All samples were filtered through a 0.45-μm Whatman Autovial poly(tetrafluoroethylene) filter before analysis. Inductively coupled plasma (ICP; Perkin-Elmer Optima 3000DV) was used for measuring the total iron and chromium concentrations. The concentrations of Cr(VI) and Fe(II) were analyzed colorimetrically using a Shimadzu 1240 UV−vis spectrophotometer. Cr(VI) was analyzed using the 1,5-diphenylcarbazide method,[21] and Fe(II) was analyzed using the Ferrozine method.[22] The ferric ion concentration was obtained by subtracting the ferrous ion concentration from the total iron concentration measured by ICP. The Cr(III) concentration was obtained by subtracting the Cr(VI) concentration from the total chromium concentration. The p*I* of the TiO_2 particles in water was determined using a Brookhaven ZetaPlus ζ potential analyzer. Experimental TiO_2 suspensions for ζ potential analysis were prepared in ultrapure water. X-ray photoelectron spectroscopy (XPS) was performed on the AXIS-His spectrometer (Kratos Analytical Ltd., Manchester, England) using a monochromatic Al Kα X-ray source (1486.6-eV photons) at a constant dwell time of 100 ms and a pass energy of 40 eV.

Results and Discussion

Effect of the pH on the Photocatalytic Reduction of Cr(VI). A series of experiments were conducted at different pH values ranging from 2.5 to 9, containing 600 μM Cr(VI) and 2 g/L of catalysts (TiO_2 or ZnO) in order to investigate photocatalytic reactions of Cr(VI). Under illumination with the UV lamp, the Cr(VI) solution gradually lost its original yellow color, while the originally white TiO_2 and ZnO turned pale green. According to the preliminary thermodynamic analysis (Figure 1), the product of the TiO_2 (or ZnO) photocatalytic reduction of Cr(VI) should be Cr(III). Figure 3 shows the temporal profiles of Cr(VI) reduction by UV/TiO_2 (and UV/ZnO) at different pH values. The figure shows the change of concentration for the photocatalytic reduction only (i.e., the results shown are obtained after it was ascertained that an adsorption equilibrium has been attained and the lamp was turned on) and indicates that reduction rates increase with decreasing pH. Because $Cr_2O_7^{2-}$ ions are the predominant species at medium to low pH values, the reduction of Cr(VI) by

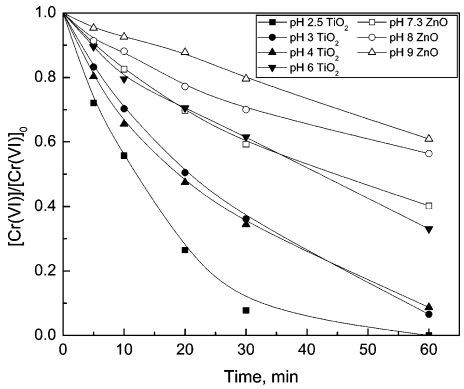

Figure 3. Photocatalytic reduction of Cr(VI) in a slurry system. Experimental conditions: [catalyst] = 2 g/L, $[Cr(VI)]_0 = 550\ \mu M$, [HCOOH] = 20 mM.

Table 1. Percentage of Cr(VI) Adsorbed on Catalysts at Different pH Values (Initial Cr(VI) Concentration = 0.6 mM; Dose of the Catalyst = 2 g/L)

catalyst	pH	Cr(VI) adsorbed (%)	k_{ads} (min^{-1})
TiO_2	2.5	24.4	0.0302
	3	12.3	0.0273
	4	12.4	0.0217
	6	6.4	0.0119
ZnO	7.3	5.8	
	8	3.6	
	9	2.7	

photogenerated electrons can be described as follows:

$$Cr_2O_7^{2-} + 14H^+ + 6e^- \rightleftharpoons 2Cr^{3+} + 7H_2O \qquad (1)$$

On the basis of the trends in Figure 1, the reduction potential of the $Cr_2O_7^{2-}/Cr^{3+}$ couple shifts 138 mV per pH unit to more cathodic potentials, whereas the conduction band of the semiconductor shifts 59 mV per pH.[17] Consequently, the thermodynamic driving force for the reduction of Cr(VI) decreases by 79 mV with an increase of pH by one unit. The decreasing reaction rate may also be attributed to the deposition of $Cr(OH)_3$ on the catalyst surface at pH values above 5. It has also been reported[7] that TiO_2 may deactivate at pH >4.5.

The kinetic experiments were conducted at different pH media to study the adsorption behavior of Cr(VI) on TiO_2 particles as well as on ZnO particles. The experimental results shown in Table 1 indicate that the adsorptivity of Cr(VI) decreases with increasing pH. The trend is consistent with that reported by Prairie et al.[3] Because the initial concentration of Cr(VI) involved in this study was low, the adsorption kinetics can be described by a simplified first-order rate equation:

$$-\frac{d[Cr(VI)]}{dt} = k_{ads}C \qquad (2)$$

$$\ln(C_{A0}/C_A) = k_{ads}t \qquad (3)$$

where k_{ads} is the adsorption constant and C_{A0} and C_A are the Cr(VI) concentrations at the initial time and time t. The k_{ads} values are listed in Table 1. Generally, the kinetics of the photocatalytic reaction follow a Langmuir−Hinshelwood mechanism in heterogeneous media, with the initial rate, r, being

$$r = k\frac{KC}{1 + KC} \qquad (4)$$

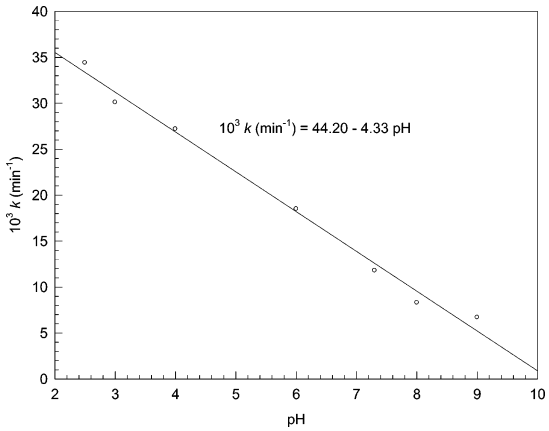

Figure 4. Dependence of the reaction rate constant on pH. Experimental conditions: same as those in Figure 3.

Table 2. First-Order Reduction Rate Constants of Cr(VI) by UV/TiO_2 (or UV/ZnO) at Different pH Values

catalyst	pH	k_{rxn} (min^{-1})	r^2
TiO_2	2.5	0.0346	0.995
	3	0.0303	0.974
	4	0.0274	0.994
	6	0.0188	0.989
ZnO	7.3	0.0137	0.991
	8	0.0091	0.987
	9	0.0073	0.993

where K is taken to represent the Langmuir adsorption constant, k is a "reactivity constant", providing a measure of the reactivity of the catalyst surface with the substrate, and C is the initial concentration of the substrate. For dilute solutions, such as 6×10^{-4} M in this study, the reaction could be reduced to first order, with kK being the rate constant:

$$\ln(C_{A0}/C_A)t = kKt = k_{rxn}t \qquad (5)$$

The k_{rxn} values of the Cr(VI) reduction with r^2 of linear regression at different pH media are listed in Table 2. The pH effect on the photocatalytic reduction of Cr(VI) is somewhat similar to the adsorption of Cr(VI) on TiO_2 particles. Furthermore, the comparable rate constants for photocatalytic reduction and adsorption of Cr(VI) indicate that adsorption of Cr(VI) is the rate-determining step.

Although the photocatalytic reduction of Cr(VI) in TiO_2 suspensions is favored at low pH, the case for ZnO is different from that for TiO_2. Because ZnO, unlike TiO_2, can partially dissolve in an acidic solution and be photodecomposed to Zn(II)[13]

$$ZnO + 2h^+ \rightarrow Zn(II) + \frac{1}{2}O_2 \qquad (6)$$

experiments involving ZnO were carried out in a basic solution. As shown in Figure 1, at high pH values, the thermodynamic driving force for the reduction of Cr(VI) by ZnO is much smaller than that by TiO_2 and the Cr(VI) adsorption on ZnO (shown in Table 1) was less than that on TiO_2. Thus, the rate of Cr(VI) photoreduction in a ZnO suspension being lower than that in a TiO_2 suspension (Figure 3) can be ascribed to the pH value. Moreover, it has been observed that Zn^{2+} is produced at pH 7.3 as a result of ZnO photocorrosion.

The results reported in Figure 3 were found to follow first-order rate dependence. The first-order reaction rate constant, k_{rxn} (min^{-1}), were determined for each pH by

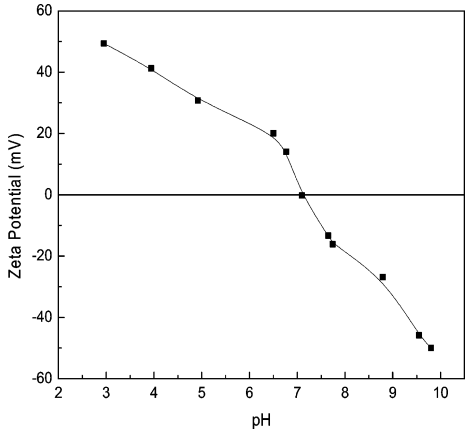

Figure 5. ξ potential of TiO_2 suspensions as a function of pH at an ionic strength ($NaNO_3$) of 0.001 M.

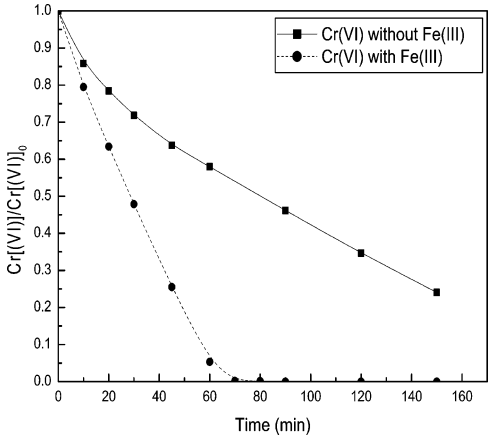

Figure 6. Influence of Fe(III) on the temporal profiles of Cr(VI) reduction. Experimental conditions: $[TiO_2] = 0.4$ g/L, $[Cr(VI)]_0 = 550$ μM, $[Fe^{3+}] = 600$ μM, [HCOOH] = 20 mM, pH 2.5.

least-squares regression, and the results are shown in Figure 4. It was observed that the reaction rate constant decreases linearly with an increase of the pH, and the pH dependence is given by

$$k\ (\mathrm{min}^{-1}) = 0.0442 - 0.00433\mathrm{pH} \qquad (7)$$

Effect of HCOOH on the Photocatalytic Reduction of Cr(VI). Previous studies[5,23,24] on the influence of organic additives on metal ion reduction in UV-irradiated TiO_2 suspensions reveal that the photoreduction of metal ions can occur by two pathways: One is a direct pathway where metal ions are reduced by reaction with the conduction band electrons on the TiO_2 surface; another is an indirect pathway where metal ions are reduced by aqueous radical species. The following steps create these radicals:

$$TiO_2 \xrightarrow{h\nu} h^+ + e^- \qquad (8)$$

$$h^+ + RH \rightarrow {}^{\bullet}R + H^+ \qquad (9)$$

$$h^+ + H_2O \rightarrow {}^{\bullet}OH + H^+ \qquad (10)$$

$${}^{\bullet}OH + RH \rightarrow {}^{\bullet}R + H_2O \qquad (11)$$

where h^+ is the hole generated on the TiO_2 surface. Organic radicals, such as $^{\bullet}R$, are normally highly reducing.[23] For example, the reduction potential of $HCOO^{\bullet}/CO_2$ is -1.7 V vs SHE,[24] which is negative enough to reduce Cr(VI).

Generally, the adsorption is mainly attributed to the surface properties of the substrate. TiO_2 Degussa P25 has been reported as a nonporous mixture of anatase and rutile with a mass ratio[1] of 70:30. The ξ potential values of Degussa P25 in an aqueous solution as a function of pH are presented in Figure 5. The isoelectric point, p*I*, was ~7.2. This is in agreement with the value of the point of zero charge (around pH 6.7−7.5).[8,25] Consequently, it can be assumed that the amount of positive charges on the TiO_2 surface decreases with increasing pH until reaching zero at pH 7.2. For solution pH greater than 6, the groups with negative charges on the TiO_2 surface are assumed to increase gradually; hence, both Cr(VI) oxyanions and $COO^{\bullet-}$ ($pk_a[HCOO^{\bullet}/COO^{\bullet-}] = 1.4$) are repelled, and the adsorption is reduced at higher pH values. The high pH has a negative effect on the Cr(VI) reduction through direct electron transfer on the surface of TiO_2 due to the electrostatic repulsion between TiO_2 particles and Cr(VI) oxyanions. On the contrary, the rate of Cr(VI) reduction by free radicals increases as a result of more free $COO^{\bullet-}$ repulsed by TiO_2 particles in the bulk solution. Figure 3 shows the reduction rate of Cr(VI) decreasing by increasing pH regardless of the increase of $COO^{\bullet-}$ in the bulk solution. Thus, the influence of pH on Cr(VI) photocatalytic reduction suggests that photocatalytic reduction of Cr(VI) is mainly through direct electron transfer on the surface of TiO_2. In Table 1, the difference of Cr(VI) adsorption between pH 3 and 4 was not significant, which is consistent with the photocatalytic reduction of Cr(VI) at pH 3 and 4 (Figure 3). A similar effect of pH on Cr(VI) photocatalytic reduction and adsorption also indicates that conduction band electrons on the surface of TiO_2 make a predominant contribution to Cr(VI) reduction. In other cases, the reduction of Ni(II) by photoinduced radicals, such as $HCOO^{\bullet}$ and $CH_3CH_2O^{\bullet}$, has been reported.[26] However, the rate of such a reaction was found to be too low here. Hence, formic acid enhances the photoreduction rate mainly by suppressing electron−hole recombination on the TiO_2 surface and not by producing radicals.

Effect of Ferric Ion on Cr(VI) Reduction. Figure 6 shows the Cr(VI) reduction profiles at pH 2.5 with 0.4 g/L of TiO_2 in the absence and in the presence of Fe(III). The rather dramatic effect of ferric ions on the Cr(VI) reduction profile can be seen. Similar results were reported for the reduction of Cr(VI) by the UV/TiO_2 process for solution pH between 4 and 8 by Munoz and Domenech.[25] They assumed that the higher yield obtained for the Cr(VI) photoreduction was due to the iron(III) and chromium(III) hydroxides, which can maintain the pH during the whole process. However, the formation of hydroxides can be ruled out because the aqueous solution in our experiments was maintained at pH 2.5. Previous authors[4] have reported that a ferrous ion generated by a photocatalytic reduction of Fe(III) had a promoting effect on the reduction of Hg(II) in illuminated TiO_2 systems. To further prove that this mechanism is operative here, the reduction of Fe(III) in the Cr(VI)/TiO_2 photocatalysis system was measured (Figure 7). As the Cr(VI) concentration decreased toward zero upon UV irradiation, the ferric ion level remained almost constant initially and then decreased when the Cr(VI) concentration was very low. The reduction of Fe(III) in this system is somewhat different from photocatalytic reduction of Fe(III) in the absence of Cr(VI) (Figure 7). Table 3 summarizes Fe(III) removal

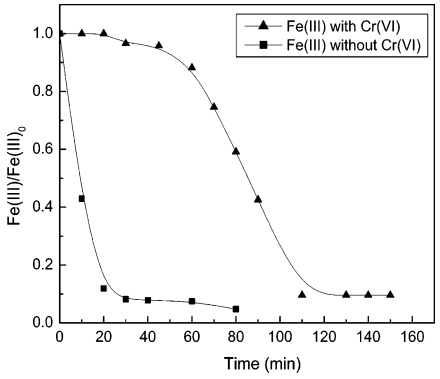

Figure 7. Temporal profiles of Fe(III) reduction in the UV/TiO_2 process. Experimental conditions: $[TiO_2] = 0.4$ g/L, $[Fe^{3+}]_0 = 600$ μM, [HCOOH] = 20 mM, pH 2.5.

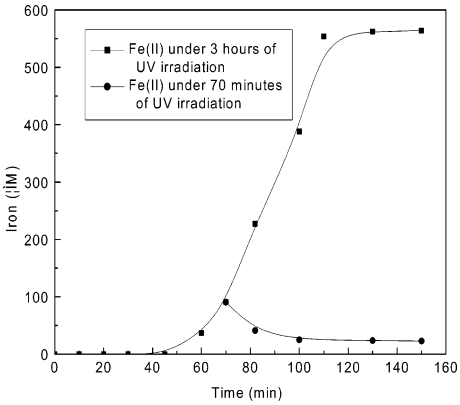

Figure 8. Identification of reaction (12) occurring during Cr(VI) photocatalytic reduction. Experimental conditions: $[TiO_2] = 0.4$ g/L, $[Fe^{3+}] = 600$ μM, [HCOOH] = 20 mM, pH 2.5.

Table 3. Percentage of Fe(III) Adsorbed on TiO_2 at Different pH Values (Initial Fe(III) Concentration = 0.6 mM; Dose of the TiO_2 = 2 g/L)

pH	Fe(III) adsorbed (%)	pH	Fe(III) adsorbed (%)
3	93.5	4.5	99.8
	94.6[a]	6	100

[a] 0.6 mM Cr(VI) was also present.

by adsorption only. This demonstrates that TiO_2 has very high adsorption capacities for Fe(III) (compared to Cr(VI) shown in Table 1) and an adsorption equilibrium could be established within a few minutes. Therefore, when both Cr(VI) and Fe(III) are present in the solution, Fe(III) is preferably adsorbed on TiO_2 and, subsequently, photoreduced to Fe(II) on the surface of the catalyst. However, what made the Fe(III) concentration constant in the Cr(VI)/UV−TiO_2 system? Figures 6 and 7 indicate that Fe(II) generated by photocatalytic reduction of Fe(III) on the surface of TiO_2 may be consumed by the thermal reduction of Cr(VI) in the bulk solution. In the presence of Fe(III), Cr(VI) is reduced via two pathways: (a) by surface reaction (1) as mentioned before and (b) by the following redox reactions:

$$\mathrm{Fe(III)} + \mathrm{e}^- \xrightarrow{\mathrm{TiO_2},\, h\nu} \mathrm{Fe(II)} \qquad (12)$$

$$3\mathrm{Fe(II)} + \mathrm{Cr(VI)} \rightarrow 3\mathrm{Fe(III)} + \mathrm{Cr(III)} \qquad (13)$$

Reactions (12) and (13) were supported[27] by the experiment considered in Figure 8. A photocatalysis experiment was carried out at pH 2.5 with initial concentrations of 600 μM Fe(III) and 600 μM Cr(VI);

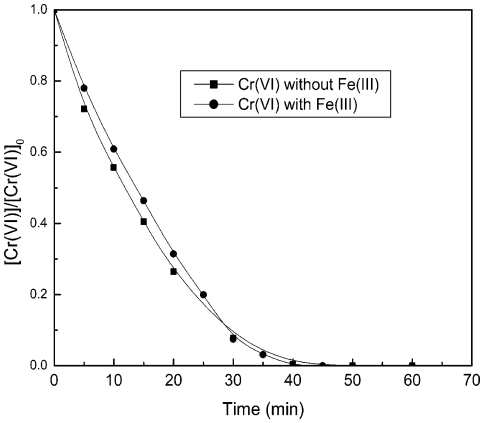

Figure 9. Influence of Fe(III) on the temporal profiles of Cr(VI) reduction. Experimental conditions: $[TiO_2] = 2$ g/L, $[Cr(VI)]_0 = 450$ μM, $[Fe^{3+}] = 600$ μM, [HCOOH] = 20 mM, pH 2.5.

after 70 min of UV irradiation, the light was cut off. The behavior of Fe(II) was completely different from the case under the UV irradiation for 3 h, which is illustrated in Figure 8. The homogeneous reaction between Fe(II) and Cr(VI) under UV illumination demonstrated that the Cr(VI) concentration decreased with illumination time. Without UV irradiation, the concentration of Fe(II) decreased slowly, because it was oxidized by the residual Cr(VI). For the case when the system was still under UV irradiation after 70 min, it increased fast. When the temporal profiles of Cr(VI) reduction are compared in Figure 6, it is observed that the rates of Cr(VI) reduction during the first 10 min were almost the same. This indicates that reaction (13) took place only after an appreciable amount of Fe(II) was formed (i.e., after ~10 min).

Figure 9 shows the Cr(VI) reduction profiles at pH 2.5 with 2 g/L of TiO_2 in the absence and in the presence of Fe(III). Unlike the earlier experiments in Figure 6 (where the dosage of TiO_2 was 0.4 g/L), the influence of Fe(III) on the reduction of Cr(VI) was found to be insignificant. It was observed that the rate of Cr(VI) photocatalytic reduction is affected by the dosage of the TiO_2 catalyst. In this case with a relatively large surface area of catalyst available for adsorption, both Fe(III) and Cr(VI) are adsorbed. Because the reduction potentials of both Fe(III)/Fe(II) and Cr(VI)/Cr(III) couples are of comparable value at pH 3, both Fe(III) and Cr(VI) are photoreduced at the same time. Moreover, the profiles of Cr(VI) reduction in the absence of Fe(III) in Figures 6 and 9 show that the reduction rate of Cr(VI) is much higher with 2 g/L of TiO_2 than with 0.4 g/L. It has been previously reported that an optimum TiO_2 dosage[7] was ~2 g/L, while it was 5 g/L for CdS.[15] The pseudo-first-order reduction rate constant of Cr(VI) with 2 g/L of TiO_2 at pH 2.5 reported as 0.0048 min^{-1} is much larger than that of Cr(VI) reduction by a ferrous ion, which was reported as 0.0017 min^{-1}, when the concentration of the ferrous ion was 100 μM.[8,28] Therefore, the positive effect from the ferrous ion is very small and negligible when the TiO_2 dose is near the optimum value of 2 g/L.

Effect of Oxygen on Cr(VI) Reduction. Table 4 contains data from two photocatalysis experiments at pH 2.5, where N_2 and air were used as the purge gas. Experiments were carried out under identical conditions for the 1-h adsorption and the 3-h photocatalytic reduction. Initial concentrations of Cr(VI) and Fe(III) were 600 μM. The TiO_2 dosage was 0.4 g/L, while formic acid at 20 mM was used as the hole scavenger.

Table 4. Influence of Oxygen on the Photocatalytic Reduction of Cr(VI) and Fe(III) (over 3 h of UV Irradiation)

	ions reduced (%)	
metal ions	in an open system	in a N_2-purged system
Cr(VI)	100	100
Fe(III)	90.6	92.3

Table 5. Cr(VI) Removal by Photocatalytic Reduction Followed by Coprecipitation

treatment details	total Cr (ppm)	total Zn (ppm)	total Fe (ppm)
initial concentration	31.2	83.8	33.5
photocatalytic reduction at pH 2.5 for 50 min[a]	10.7	62.2	18.9
coprecipitation at pH 7.26	0.017	32.4	0.058
Zn removal at pH 10.08	0.012	0.038	0.037

[a] $[TiO_2] = 2$ g/L.

The amount of Fe(III) and Cr(VI) photoreduced in an air-equilibrated system and a N_2-purged system indicates that the reaction is not significantly influenced by oxygen. Opposite results of Cr(VI) photocatalytic reduction at pH 10 were reported by Wei et al.[29] This may be explained by the fact that the thermodynamic driving forces for the reduction of Cr(VI) and O_2 depend on pH. It is clearly shown in Figure 1 that the thermodynamic driving forces are similar for the reduction of Cr(VI) and O_2 at pH 2.5. However, at pH 10, the thermodynamic driving force for O_2 is much higher than that for Cr(VI) and consequently oxygen competes with Cr(VI) for the photogenerated electrons. In the case of Fe(III), significant adsorption of Fe(III) on TiO_2 helps it to be reduced by conduction band electrons, e_{cb}^-.

Removal of Cr(VI) from Simulated Leather Tanning Waste. On the basis of a literature survey regarding heavy-metal adsorption by ferric hydroxide,[30] a combination of photocatalytic reduction and metal ion coprecipitation was used to remove aqueous Cr(VI) from the simulated leather tanning industry. The sample that simulated waste from the leather tanning industry contained ~30 ppm of Cr(VI), 80 ppm of Zn(II), and 30 ppm of Fe(III). Following the photocatalytic reduction in TiO_2 suspensions at pH 2.5, the pH of the solution was adjusted to approximately 7 and the sample was allowed to settle following 1 h of flocculation. The supernatant samples were tested, with the results shown in Table 5. To achieve the complete removal of Zn as well as Cr, the pH of the supernatant samples was then raised to ~10.

As can be seen, the chromium concentration was reduced below the water quality criterion established by the U.S. EPA.[31] Actually, it is comparable to the most widely used method using iron to reduce chromium to the trivalent state.[32,33] The advantage of the combination of photocatalytic reduction and metal ion coprecipitation over other treatment methods is that it only took ~2 h for the entire process to remove 30 ppm of chromium with the same dose of iron. The amount of ferrous ions added to the Cr(VI)-contaminated water was kept in excess of the stoichiometric ratio of 3.2 lb of iron/lb of chromium in the treatment reported by El-Shoubary et al.[32] Although Blowes et al.[33] described in situ permeable reactive barriers containing Fe^0 to remove dissolved Cr(VI) from groundwater, the ferric oxyhydroxide precipitation during the process limited the available surface area of the reactive barrier, which would inhibit Cr(VI) reduction.

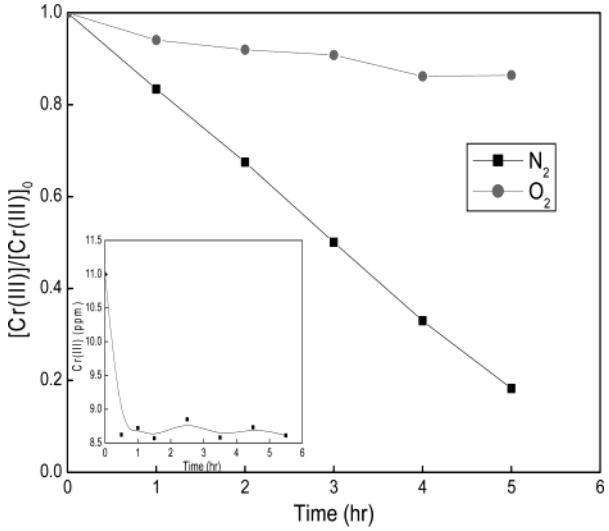

Figure 10. Photocatalytic reduction of Cr(III) in ZnS suspensions. Experimental conditions: $[ZnS] = 8$ g/L, $[Cr(III)]_0 = 8.5$ ppm, $[HCOOH] = 20$ mM, pH 5.2 Inset: adsorption of Cr(III) on ZnS in the dark.

Table 6. Conditions for Cr(III) Removal[a]

formic acid	UV irradiation[b]	ZnS	% Cr(III) removed
√	√	×	0
√	×	√	21
×	√	√	71
√	√	√	86

[a] Conditions: Cr(III) (210 μM), formic acid (20 mM), and ZnS (8 g/L): √ indicates the presence of the component; × indicates the absence of the component. [b] After 5 h of irradiation.

Photocatalytic Reduction of Cr(III). Preliminary thermodynamic analysis (see Figure 1) reveals that photogenerated electrons in ZnS are capable of reducing Cr(III). Considering that Cr(III) is positively charged and that adsorption on the ZnS surface is favored in basic aqueous solutions, the experiments were conducted at pH ~5. Figure 10 shows the Cr(III) temporal profile in a solution containing 11 ppm of Cr(III). The rate of Cr(III) concentration decrease was found to be low in an open system (O_2 saturated); however, the rate was greatly enhanced in the N_2-purged system. This increase in rate indicates that Cr(III) photoreduction is inhibited in the presence of oxygen. This is because oxygen, whose reduction potential ($E^0 = 1.0$ V at pH 5) is much higher than that of Cr(III) ($E^0 = -0.79$ V at pH 5), competes with Cr(III) ions for the photogenerated electrons.

Interestingly, the data in the N_2-purged system exhibit zero-order kinetics, which is different from the reduction reaction of Cr(VI) by a TiO_2 photocatalyst. Because the inset in Figure 10 shows that adsorption of Cr(III) on ZnS is fast, Cr(III) adsorption on ZnS was allowed to reach an equilibrium in 1 h before the photocatalytic reaction. Meanwhile, electron transfer from ZnS to Cr(III) is more difficult than electron transfer from TiO_2 to Cr(VI) because of the small difference between the ZnS conduction band edge and the reduction potential of Cr(III). Therefore, the rate-determining step here may be the electron transfer from ZnS to Cr(III), not the adsorption of Cr(III).

The appearance of black particles in the suspension reveals that they were presumably metallic Cr. To ensure that Cr(VI) was not formed, chromium adsorbed on ZnS was desorbed at alkaline conditions after UV

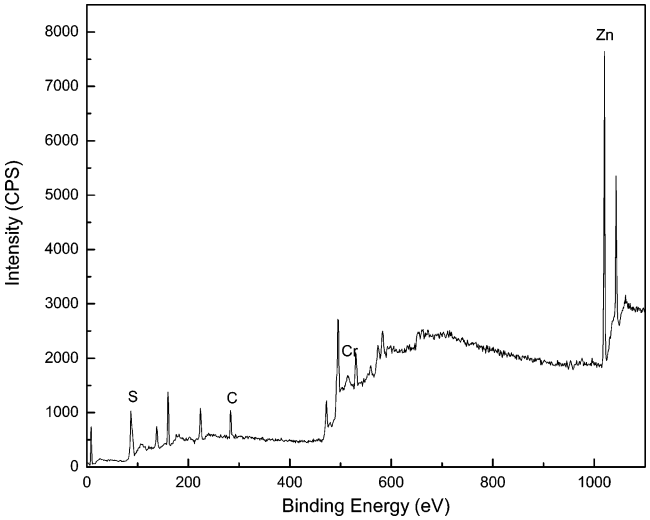

Figure 11. XPS spectrum of a ZnS sample after photocatalytic reduction of Cr(III).

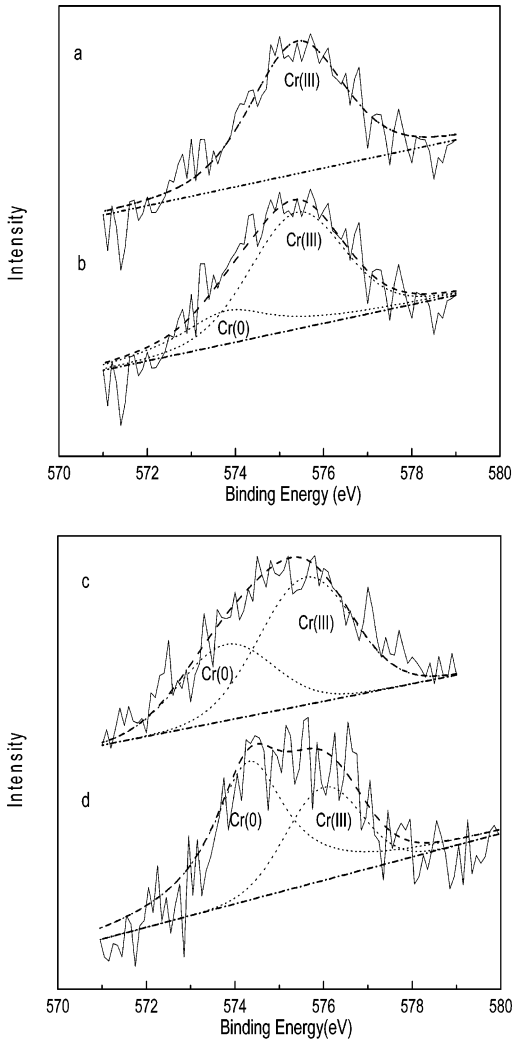

Figure 12. XPS spectra of Cr on the ZnS surface: (a) $CrCl_3$ in the dark reaction, 0.5 h; (b) $CrCl_3$ in the dark reaction, 5 h; (c) $CrCl_3$ under 2.5 h of UV irradiation; (d) $CrCl_3$ under 5 h of UV irradiation.

irradiation and no Cr(VI) was detected using the diphenylcarbazide method. Other control experiments are summarized in Table 6. These demonstrate that ZnS, light, and formic acid are all required for the effective removal of Cr(III).

To further identify the photoreduction of Cr(III) on the surface of ZnS, the ZnS powders after photocatalysis were investigated by XPS. A wide scan of the ZnS powder is shown in Figure 11. High-resolution scans of Cr $2p_{3/2}$ peaks are shown in Figure 12. In Figure 12a, a single peak after 30 min of dark reaction is located at 575.6 eV, which is assigned to Cr(III). After 5 h of dark reaction (Figure 12b), there are overlapping peaks of two different chromium species, one of which is in the peak position of Cr(III) and the other of which shifts to 573.8 eV, which is expected to be elemental Cr.[34] Parts c and d of Figure 12 show the same system as in those in parts a and b of Figure 12 but after different periods of UV irradiation. The peak width at half-maximum and the peak height for Cr(0) appear narrower and sharper, respectively, with the longer period of UV irradiation, indicating that Cr(III) on the ZnS surface is increasingly reduced to Cr(0).

Conclusions. Both the thermodynamic and kinetic analyses show that the photocatalytic reduction of Cr(VI) under UV-A irradiation depends largely on pH. The reaction occurs on the surface of TiO_2 by directly capturing photogenerated electrons. Ferric ions are shown to exert a dramatic accelerating influence on Cr(VI) reduction, which can be accomplished within 90 min when the TiO_2 dose was as low as 0.4 g/L. However, the presence of oxygen does not affect the reduction of Cr(VI) and Fe(III) in acidic solutions because of the high reduction potential of Cr(VI) and a significant adsorption of Fe(III) onto TiO_2. Because TiO_2 can only photoreduce Cr(VI) to Cr(III), a new process for removing aqueous Cr(VI) using photocatalytic reduction followed by coprecipitation with ferric ions proved successful. Finally, it was found out that ZnS can be used as a photocatalyst for further reduction of Cr(III) to Cr(0).

Literature Cited

(1) Hoffmann, M. R.; Martin, S. T.; Choi, W.; Bahnemann, D. W. Environmental Applications of Semiconductor Photocatalysis. *Chem. Rev.* **1995**, *95*, 69.

(2) Tryk, D. A.; Fujishima, A.; Honda, K. Recent topics in photo electrochemistry: achievements and future prospects. *Electrochim. Acta* **2000**, *45*, 2363.

(3) Prairie, M. R.; Evans, L. R.; Stange, B. M.; Martinez, S. L. An Investigation of TiO_2 Photocatalysis for the Treatment of Water contaminated with Metals and Organic Chemicals. *Environ. Sci. Technol.* **1993**, *27*, 1776.

(4) Chen, D.; Ray, A. K. Removal of Toxic Metal Ions from Wastewater by Semiconductor Photocatalysis. *Chem. Eng. Sci.* **2001**, *56*, 1561.

(5) Yang, H.; Lin, W.-Y.; Rajeshwar, K. Homogeneous and Heterogeneous Photocatalytic Reactions Involving As(III) and As(V) Species in Aqueous Media. *J. Photochem. Photobiol., A* **1999**, *123*, 137.

(6) Lee, H.; Choi, W. Photocatalytic Oxidation of Arsenite in TiO_2 Suspension: Kinetics and Mechanisms. *Environ. Sci. Technol.* **2002**, *36*, 3872.

(7) Aguado, M. A.; Gimenez, J.; Cervera-March, S. Continuous Photocatalytic Treatment of Cr(VI) Effluents with Semiconductor Powders. *Chem. Eng. Commun.* **1991**, *104*, 71.

(8) Ku, Y.; Jung, I.-L. Photocatalytic Reduction of Cr(VI) in Aqueous Solutions by UV Irradiation with the Presence of Titanium Dioxide. *Water Res.* **2001**, *35*, 135.

(9) Chenthamarakshan, C. R.; Rajeshwar, K. Heterogeneous Photocatalytic Reduction of Cr(VI) in UV-Irradiated Titania Suspensions: Effect of Protons, Ammonium Ions, and Other Interfacial Aspects. *Langmuir* **2000**, *16*, 2715.

(10) Navío, J. A.; Colón, G.; Trillas, M.; Peral, J.; Domenech, X.; Testa, J. J.; Padrón, J.; Rodríguez, D.; Litter, M. I. Heterogeneous Photocatalytic Reactions of Nitrite Oxidation and Cr(VI) Reduction on Iron-doped Titania Prepared by the Wet Impregnation Method. *Appl. Catal., B* **1998**, *16*, 187.

(11) Testa, J. J.; Grela, M. A.; Litter, M. I. Experimental Evidence in Favor of an Initial One-Electron-Transfer Process in the Heterogeneous Photocatalytic Reduction of Chromium(VI) over TiO_2. *Langmuir* **2001**, *17*, 3515.

(12) Selli, E.; Giorgi, A. D.; Bidoglio, G. Humic Acid-Sensitized Photoreduction of Cr(VI) on ZnO Particles. *Environ. Sci. Technol.* **1996**, *30*, 598.

(13) Khalil, L. B.; Mourad, W. E.; Rophael, M. W. Photocatalytic Reduction of Environmental Pollutant Cr(VI) over Some Semiconductors under UV/Visible Light Illumination. *Appl. Catal., B* **1998**, *17*, 267.

(14) Bidoglio, G.; Ferrari, D.; Selli, E.; Sena, F.; Tamborini, G. Humic acid binding of trivalent Tl and Cr studied by synchronous and time-resolved fluorescence. *Environ. Sci. Technol.* **1997**, *31*, 3536.

(15) Wang, S.; Wang, Z.; Zhuang, Q. Photocatalytic Reduction of the Environmental Pollutant Cr^{VI} over a Cadmium Sulphide Powder under Visible Light Illumination. *Appl. Catal., B* **1992**, *1*, 257.

(16) Dean, J. A. *Lange's Handbook of Chemistry*, 14th ed.; McGraw-Hill: New York, 1992.

(17) Xu, Y.; Schoonen, M. A. A. The Absolute Energy Positions of Conduction and Valence Bands of Selected Semiconducting Minerals. *Am. Mineral.* **2000**, *85*, 543.

(18) Blowes, D. Environmental chemistry—Tracking hexavalent Cr in groundwater. *Science* **2002**, *295*, 2024.

(19) Pehkonen, S. O.; Lin, C. J. Aqueous photochemistry of mercury with organic acids. *J. Air Waste Manage. Assoc.* **1998**, *48*, 144.

(20) Chen, J.; Pehkonen, S. O.; Lin, C.-J. Degradation of monomethylmercury chloride by hydroxyl radicals in simulated natural waters. *Water Res.* **2003**, *37*, 2496.

(21) Ueno, K.; Imamura, T.; Cheng, K. L. *Handbook of organic analytical reagents*; CRC Press: Boca Raton, FL, 1992; p 339.

(22) Stookey, L. L. Ferrozine: A new spectrophotometric reagent for iron. *Anal. Chem.* **1970**, *42*, 779.

(23) Wardman, P. Reduction Potentials of One-electron Couples Involving Free-radicals in Aqueous Solution. *J. Phys. Chem. Ref. Data* **1989**, *18*, 1637.

(24) Chenthamarakshan, C. R.; Rajeshwar, K. Photocatalytic Reduction of Divalent Znic and Cadmium Ions in Aqueous TiO_2 Suspensions: An Interfacial Induced Adsorption-Reduction Pathway Mediated by Formate Ions. *Electrochem. Commun.* **2000**, *2*, 527.

(25) Munoz, J.; Domenech, X. TiO_2 Catalysed Reduction of Cr(VI) in Aqueous Solutions under Ultraviolet Illumination. *J. Appl. Electrochem.* **1990**, *20*, 518.

(26) Forouzan, F.; Richards, T. C.; Bard, A. J. Photoinduced Reaction at TiO_2 Particles. Photodeposition from Ni^{II} Solutions with Oxalate. *J. Phys. Chem.* **1996**, *100*, 1812.

(27) Schlautman, M. A.; Han, I. Effects of pH and dissolved oxygen on the reduction of hexavalent chromium by dissolved ferrous iron in poorly buffered aqueous systems. *Water Res.* **2001**, *35*, 1534.

(28) Sedlak, D. L.; Chan, P. G. Reduction of Hexavalent Chromium by Ferrous Iron. *Geochim. Cosmochim. Acta* **1997**, *61*, 2185.

(29) Lin, W.-Y.; Wei, C.; Rajeshwar, K. Photocatalytic Reduction and Immobilization of Hexavalent Chromium at Titanium Dioxide in Aqueous Basic Media. *Electrochem. Soc.* **1993**, *140*, 2477.

(30) Namasivayam, C.; Ranganathan, K. Removal of Cd(II) from Wastewater by Adsorption on "Waste" Fe(III)/Cr(III) Hydroxide. *Water Res.* **1995**, *29*, 1737.

(31) *National Recommended Water Quality Criteria-Correction*; U.S. Environmental Protection Agency Report EPA-822-Z-99-001; U.S. Government Printing Office: Washington, DC, Apr 1999.

(32) El-Shoubary, Y.; Speizer, N.; Seth, S.; Savoia, H. A pilot plant to treat chromium-contaminated groundwater. *Environ. Prog.* **1998**, *17*, 209.

(33) Blowes, D. W.; Ptacek, C. J.; Jambor, J. L. In-situ Remediation of Cr(VI)-contaminated Groundwater Using Permeable Reactive Walls: Laboratory Studies. *Environ. Sci. Technol.* **1997**, *31*, 3348.

(34) Stypula, B.; Stoch, J. The Characterization of Passive Films on Chromium Electrodes by XPS. *Corros. Sci.* **1994**, *36*, 2159.

Received for review July 10, 2003
Revised manuscript received January 27, 2004
Accepted January 28, 2004

IE030580J